A model of oxidation in pyritic mine wastes: part 3: import of particle size distribution

G. B. Davis*

Department of Mathematics, University of Wollongong, P.O. Box 1144, Wollongong, NSW, 2500, Australia

A. I. M. Ritchie

Australian Atomic Energy Commission, Lucas Heights Research Laboratories, Private Mail Bag, Sutherland, NSW, 2232, Australia

(Received February 1986; revised February 1987)

An earlier mathematical model, developed to describe oxidation of pyritic material in mine wastes and which assumed just one size for the particles composing the wastes, has been extended to take proper account of the range of particle sizes in the wastes. Comparison of the simpler model with the more realistic model shows that for practical purposes the simpler model is good enough to assess the magnitude and longevity of the environmental impact of pollutant generation in the wastes. It is, however, essential to include the particle size distribution to obtain accurate estimates of the heat source distribution profile and to a lesser extent the oxygen concentration profile, two parameters that can be measured and used to assess the applicability of the model to the real field situation.

Keywords: pyritic; dump; leaching; diffusion; particle distribution

Introduction

In two earlier papers[1,2] an approximate analytical solution and a numerical solution were presented for a mathematical model developed to describe oxidation of pyritic material in large dumps of mine wastes. The model assumed that the oxidation rate was limited only by the rate of supply of oxygen to the oxidation sites and that oxygen transport was by diffusion through the pore space of the dump material followed by diffusion into reaction sites within the particles comprising the dump. Comparison was made with a simpler model (SHM) where the waste dump was assumed to be a homogeneous slab.[3] To allow proper comparison between these three approaches, we restricted modelling to the case where there was just one particle size in the dump.

In the present paper the model is extended to include the situation where there is a range of particle sizes in the dump material. This is clearly a more realistic situation since waste rock from opencut mining in particular has 'particles' ranging in size from fine grains to large boulders. Moreover Bartlett,[4] for example, found that when modelling commercial *in situ* leaching of low-grade copper ore, a process which has much in common with the oxidation of pyrite in mine wastes, the extraction rate varied markedly with different particle size distributions.

Of interest is the effect that inclusion of a particle size distribution has on parameters such as the sulphate production rate and the lifetime of oxidation in the wastes, parameters which quantify the probable environmental impact of the pyritic mine wastes. Also of interest is the effect the inclusion has on parameters such as the oxygen concentration profile and the heat source distribution, parameters which can be measured and used to assess the applicability of the model to real field situations.

Incorporation of particle size distribution in the model equations

The equation describing diffusion through the pore space of the pyritic wastes[1] can be written as

$$p\frac{\partial u^*}{\partial t^*} = D_1\frac{\partial^2 u^*}{\partial x^{*2}} - q^* \qquad (1)$$

*Present address: CSIRO Division of Groundwater Research, Private Bag, P.O. Wembley, Western Australia, 6014, Australia

0307-904X/87/060417-06/$03.00

where the notation is that of Davis and Ritchie[1] and is defined at the end of the paper. For the single-size particle model (SPM), that is, where particles composing the wastes are assumed to be all of the same size,

$$q^* = 4\pi a^2 \upsilon D_2 \frac{\partial v^*}{\partial r^*}(a, x^*, t^*) \tag{2}$$

Assuming a range of particle sizes

$$q^* = \int_{a_0}^{a_n} 4\pi a^2 D_2 \frac{\partial v^*}{\partial r^*}(a, x^*, t^*)\upsilon(a)\,da \tag{3}$$

Implicit in equations (1) and (3) are the assumptions that the particle size distribution can be found in any representative volume of the wastes and that throughout this representative volume each of the different sized particles has, at its surface, the same oxygen concentration.

The parameter $\upsilon(a)\,da$ is not easily measurable. It is, however, possible to relate $\upsilon(a)\,da$ to the mass $(M(a)\,da)$ in a sample of total mass M:

$$\frac{M(a)\,da}{M} = \frac{4}{3}\pi a^3 \frac{\rho}{\rho_T}\upsilon(a)\,da \tag{4}$$

Noting that

$$\int_{a_0}^{a_n} M(a)\,d(a) = \frac{(1-p)\rho M}{\rho_T}$$

we can write equation (4) as

$$\upsilon(a)\,da = \frac{3(1-p)M(a)\,da}{4\pi a^3 \int_{a_0}^{a_n} M(a)\,da} \tag{5}$$

After making (1) and (3) dimensionless and noting the simplified relationship,[1]

$$\frac{\partial v}{\partial r}(1, x, t) = \frac{uR_a}{1-R_a}$$

we can write equation (3), via substitution of (5), as

$$q(x, t) = \frac{3u\int_{a_0}^{a_n} \frac{kR_a}{1-R_a} M(a)\,da}{\int_{a_0}^{a_n} M(a)\,da} \tag{6}$$

where R_a is meant simply to denote the dependence of $R(x, t)$ on particle size.

The full system of dimensionless equations can therefore be written as

$$\delta_1 \frac{\partial u}{\partial t} = \frac{\partial^2 u}{\partial x^2} - q(x, t) \qquad 0 < x < 1 \tag{7}$$

$$\frac{\partial R}{\partial t} = -\frac{ku}{R(1-R)} \qquad 0 < R < 1 \tag{8}$$

The boundary and initial conditions are

$$u(0, t) = 1 \qquad \frac{\partial u}{\partial x}(1, t) = 0 \tag{9}$$

$$u(x, 0) = 0 \qquad R(x, 0) = 1 \tag{10}$$

For the SPM[1]

$$q(x, t) = \frac{3kuR}{(1-R)} \tag{11}$$

whereas inclusion of a range of particle sizes enjoins use of equation (6) for $q(x, t)$. In subsequent sections we will denote equations (6) through (10) as the distributed particle size model (DPM), and the SPM is described by equations (7) through (11).

The particle size distribution

Measurements of particle radii sizes and associated masses in a sample taken from White's overburden dump at Rum Jungle,[1] at a depth of about 3 m, yield results which allow $M(a)$ to be described to good accuracy[5] by

$$M(a) = 35.12(a_0^{2.61}/a^{0.61}) \tag{12}$$

where a_0 and a are measured in millimeters. *Figure 1* illustrates the cumulative mass fraction curve corresponding to equation (12). Also illustrated in *Figure 1* are cumulative mass fractions corresponding to particle size distributions considered by Lewis and Braun[6] and Bartlett.[4] Over much of the range of particle sizes the present particle size distribution lies between the curve for the LLL–San Manuel test ore[4] and the curve for the open-pit mine waste.[6] The open-pit mine waste has a more evenly spread distribution than the test ore, with quite a large fraction of the mine wastes at the smaller-particle-size end of the range, whereas the test ore has a larger mass fraction at the larger particle size. For example, the mine waste has half of its total mass present in particles less than 20 mm in radius, whereas for the San Manuel test ore, particles larger than 50 mm in radius must be included to achieve 50% of the total ore mass. The sample from White's waste rock dump shows that half the mass is composed of particles with radii less than approximately 32 mm. It would seem therefore that expression (12) is a reasonable description of the particle size distribution within an overburden waste pile.

Substitution of (12) into (6) allows analytical integration of the denominator to give

$$q(x, t) = k_a u \int_{a_0}^{a_n} \frac{R_a}{1-R_a} a^{-2.61}\,da \tag{13}$$

where k_a is independent of the radius a.

At any given point in the dump there will be some time at which all the particles less than a certain radius will be fully oxidized. Hence in evaluating (13) at this point in space and time, we set the lower limit of integration by the radius of the fully oxidized particles. In other words $R = 0$ at this particular point in space and time. By integrating

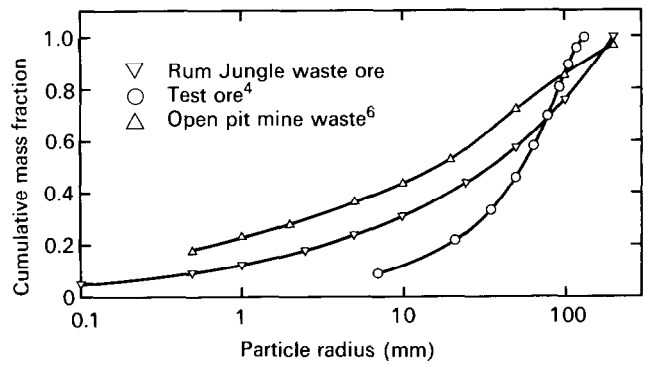

Figure 1 The particle size distribution depicted as the cumulative mass fraction versus radius size. Comparison of three ore types

equation (8) with respect to time, we have

$$3R_a^2 - 2R_a^3 - 1 + 6kw(x, t) = 0 \quad (14)$$

where $w(x, t)$ is defined by

$$w(x, t) = \int_o^t u(x, \tau)\, d\tau \quad (15)$$

When $R_a(x, t) = 0$,

$$w(x, t) = 1/6k \quad (16)$$

which from the dependence of k on a defines the lower limit of integration. It is convenient to define $k' = 3a^2k$, from which the lower limit of integration is given by

$$a_0 = (2k'w)^{1/2} \quad (17)$$

Since w is increasing with time, the integration will be over a smaller interval at each successive time step for a fixed depth in the dump.

The distributed heat source within the dump is given by

$$H(x, t) = k_H q(x, t) \quad (18)$$

where $q(x, t)$ is given by equation (13). The total sulphate production rate can be written as

$$S(t) = \frac{L\delta_s}{\delta} \int_0^1 H(x, t)\, dx \quad (19)$$

In general, the numerical technique previously developed[2] is easily extended to cope with the modified equations outlined above. To integrate over the particle size distribution in equation (13), we used a Gauss quadrature technique. The kernel of the integral was found by solving (14) for each R_a associated with each particle radius size defined by the Gauss quadrature points.

When the Gauss routine was used directly on an interval appropriate to a particle size distribution (1–200 mm, say), the particle sizes chosen by the Gauss routine tended toward the 200 mm end of the range and when used in the integration produced inaccurate results, especially for such parameters as the heat source distribution. The reason for this is apparent when we note from the SPM[1] that the smaller the particle radius size, the higher the peak of the heat source distribution, the narrower the "width", and the further down the dump the position of the peak. These observations, together with the bias of the particle size distribution towards particles of a smaller size (see *Figure 1* and expression (13)) suggest that, in order to obtain accurate information in the higher oxidation rate zone, an integration scheme accounting for the small particle size weighting of the integral kernel should be adopted. To achieve this we took the "inverse interval", that is, Gauss quadrature points were obtained for the interval $(a_n)^{-1}$ to $(a_0)^{-1}$, and the weights appropriate to the quadrature points were reweighted suitably to account for the inversion procedure. The reworking of the Gauss procedure resulted in many more points being chosen near the small-particle-size end of the range and, consequently, a more accurate estimate of parameters such as the heat source distribution.

An estimate of the starting value of a_0 may be found by considering that a particle of radius 0.5 mm is fully oxidized in about a day after it is exposed to the atmosphere under the assumptions of the present model[7]. Since the waste material forming the overburden is first excavated in the opencut and then transported to the waste rock dump site where it is back dumped on top of other waste rock, it is reasonable to suggest that all particles less than about 1 mm in radius will be fully oxidized before being covered by overburden material. Therefore for comparison with experimental data the lowest limit on a_0 is taken to be 1 mm.

Results and discussion

Results presented in *Figures 2*, *3* and *4* correspond to pyritic waste material with a pyrite content of 3.3%, a porosity of 0.4, an oxygen diffusion coefficient through the pore space of $6.72 \times 10^{-6}\ m^2\ s^{-1}$, and a depth of 18 m. These data are appropriate for White's waste rock dump at Rum Jungle in the Northern Territory of Australia.[1] Other parameters appearing in the model were set to standard values found in the literature.

Figure 2 illustrates the sulphate production rates predicted by the SHM,[3] the SPM for particle sizes 10 mm and 50 mm, and the DPM with $a_0 = 1$ mm and $a_n = 200$ mm. The sulphate production rates for all four calculations are in good general agreement. This implies that the SPM with $a = 10$ mm or 50 mm and even the SHM would be adequate, at least to engineering accuracy, in predicting the sulphate production rate from a pyritic waste rock dump.

Detailed predictions of total sulphate production rates (pollution generation rates) over the entire lifetime of the

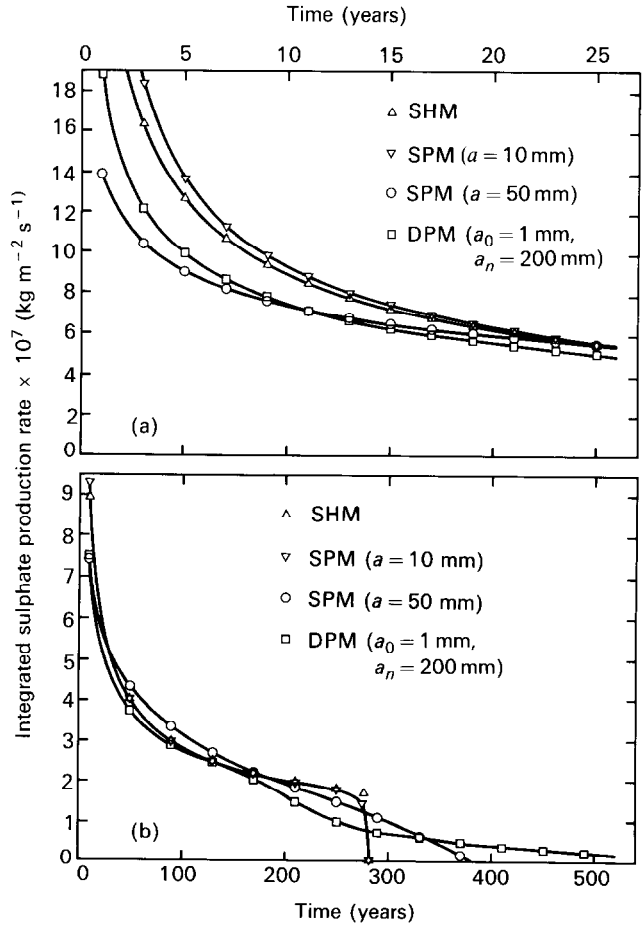

Figure 2 The total sulphate production rate as a function of time after creation of the wastes. Comparison of the SHM, SPM and DPM for (a) early time 0–26 years and (b) extended time 0–510 years

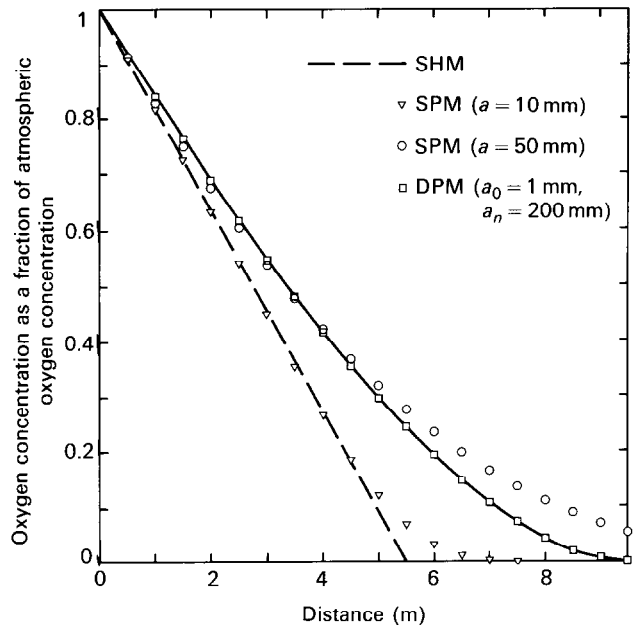

Figure 3 The dimensionless oxygen concentration as a function of distance from the surface of the wastes 26 years after creation of the wastes. Comparison of the SHM, SPM, and DPM

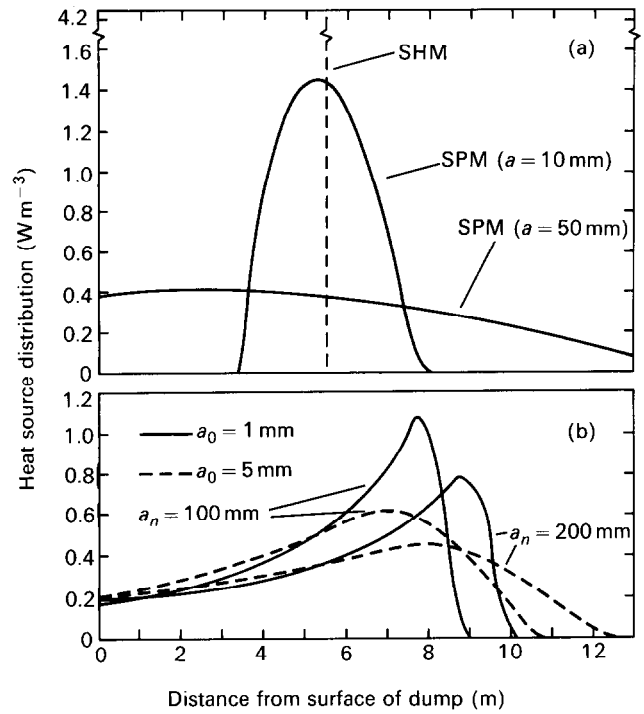

Figure 4 The spatial heat source distribution at 26 years. Comparison of (a) the SHM and SPM and (b) the DPM for $a_0 = 1$ mm (solid lines), $a_0 = 5$ mm (dashed lines) and $a_n = 100$ mm and 200 mm (as indicated)

oxidation process will, however, be inaccurate if a single "average" particle size is chosen. For example, the SPM with $a = 10$ mm best estimates the sulphate production rate predicted by the DPM between 30 and 180 years, whereas prior to 30 years (see *Figure 2(a)*) and subsequent to 180 years the sulphate production rate predicted by the DPM is best estimated by the SPM with $a = 50$ mm. We can explain this by referring to the results of Davis *et al.*[2] We know from these results that the smaller the particle the higher the oxidation rate in the pyritic material. However, there is a time beyond which all "small" particles have been fully oxidized within the dump, and thereafter it is only larger particles that contribute to the oxidation rate, with the consequence that there is a reduction in sulphate production levels. For the DPM in *Figure 2*, at about 180 years all particles no greater than 8 mm in radius are fully oxidized throughout the dump. After this time the DPM sulphate levels would be best approximated by the SPM with a larger particle size (~ 50 mm), which is confirmed by *Figure 2(b)*.

Note also the increased lifetime for the oxidation of the pyritic waste predicted by the DPM when compared with that predicted by either single-particle-size calculation. Hence, use of the SPM to predict the effective lifetime of oxidation in a pyritic waste rock pile could be misleading. The lifetime predicted by the DPM with $a_0 = 1$ mm and $a_n = 200$ mm is, however, less than the lifetime predicted by the SPM with $a = 200$ mm, since particles of a particular radius in the DPM will fully oxidize earlier than the same particle size used in an SPM calculation. For example, in the DPM with $a_0 = 1$ mm and $a_n = 200$ mm the time for particles of 30 mm radius or less to be fully oxidized is about 257 years, whereas from *Figure 2(b)* it is apparent that in the SPM with $a = 10$ mm the time to complete oxidation is about 282 years. This is due to the fractional weighting of the different particle sizes in the DPM.

The spatial distribution of oxygen within the pore space of the waste material at 26 years is depicted in *Figure 3*. Again four profiles are illustrated; the SHM, the SPM with $a = 10$ mm and 50 mm, and the DPM ($a = 1$–200 mm). Like the SHM the SPM predicts an oxygen concentration that decreases linearly with depth to the position of the moving front $X(t)$. For the SHM at 26 years $X(t) \simeq 5.5$ m, whereas for the SPM with $a = 10$ mm the depth above which particles have fully oxidized is about 3.25 m; with $a = 50$ mm no particles within the waste have fully oxidized in 26 years. In the region where particles are continuing to react, a nonlinear oxygen profile results. The DPM exhibits a nonlinear profile with depth in the dump, since, even though smaller-sized particles have been fully oxidized by this stage in the oxidation process, over the top 10 m or so of the waste dump larger particles are continuing to oxidize. Similar processes explain the higher oxygen concentrations predicted by the DPM at depths less than 3.5 m and the lower concentrations at depths greater than 3.5 m compared to those predicted by the SPM with $a = 50$ mm.

At 26 years the DPM predicts that all particles with radii less than 14 mm are fully oxidized to a depth of 3.5 m. Below this point smaller particles are still oxidizing and do so at a much greater rate than 50 mm particles. Thus the DPM predicts a greater flux of oxygen into particles comprising the waste below 3.5 m than does the SPM with a 50-mm particle. The oxygen concentration in the pore space of the material in this region of the dump is thus greater for a dump composed only of 50 mm particles. Above 3.5 m, however, only larger particles (14–200 mm) in the DPM calculation are oxidizing, the flux into the particles is lower, and the oxygen concentration in the pore space is higher compared to a dump composed only of 50-mm particles.

Figure 4 illustrates the spatial dependence of the heat source within the pyritic wastes at 26 years after the creation of the waste rock pile. Two single-particle-size

calculations and the SHM result are shown in *Figure 4(a)*. For the SPM a larger particle size results in a broader-based, less-peaked heat source distribution, with the peak of the distribution at a shallower depth. This occurs because larger particles oxidize less rapidly and are therefore fully oxidized more slowly. The SHM result is shown only to indicate the position of its peak heat production, which is the position of the moving reaction front $X(t) = 5.51$ m.

Four DPM calculations are shown in *Figure 4(b)* for differing a_0 and a_n. It is apparent that the smaller the lower cutoff radius the higher the peak and the narrower the width of the heat source distribution. This is consistent with the results of the SPM. There is, however, a very marked difference between the peak height predicted by the SPM with $a = 1$ mm, for example, and that predicted by the DPM. The heat source distribution predicted by the SPM gives a peak of 13 W m^{-3} centred around 5.5 m with a width of about 0.5 m, whereas that predicted by the DPM with $a = 1$–200 mm has a peak height of only 1.1 W m^{-3} positioned at the much greater depth of 7.75 m, with a width that extends from the surface of the dump to a depth of about 9 m. For the SPM with a larger particle size the contrast is still significant but not as great. Note especially that for the SPM with $a = 10$ mm there is no heat production down to 3.24 m below the surface, because all particles in this shallower region have been fully oxidized at 26 years. Contrariwise the heat source distribution calculated for a range of particle sizes exhibits heat production throughout the region between the high oxidation rate zone and the surface of the dump. The heat production near the surface is due to larger particles which are not fully oxidized and which are still producing heat from the oxidation of pyrites within them.

Although variations in the heat source distributions due to changes in the minimum particle size are reasonably easy to explain in terms of our experience with SPM results, it is more difficult to explain variations due to changes in the maximum particle size. We may well expect, for a larger upper limit particle size, that the maximum heat production would be reduced, and indeed this is observed in *Figure 4(b)*; however, we find also that the positioning of the peak is further down the pyritic waste than is the case for a smaller upper limit radius cutoff. This appears to contradict information in *Figure 4(a)*, which for larger particles implies a lower peak positioned closer to the surface of the waste material. This characteristic of the results can, however, be explained when we consider the effect of inclusion of additional, large particles within an elemental volume of the waste dump. Increasing a_n effectively reduces the fractional volume weighting of particles of other sizes and, in particular, reduces the volume fraction of the smallest particles. Therefore per unit volume of the wastes less time is required for the most rapidly oxidizing particles to be fully oxidized, which in turn allows the peak rate of heat production, for the larger upper limit on the particle size, to move further down into the waste dump while at the same time reducing the magnitude of the peak.

Conclusions

Over much of the lifetime of oxidation in pyritic wastes the SPM and even the SHM give the sulphate production rate to within 10–20%. In the early stages of oxidation (< 5 years) the discrepancy between the SPM and the more realistic DPM increases to more than 50%, depending on the value of the single-particle size chosen to typify particles in the wastes. Hence the SPM or SHM are almost certainly accurate enough for assessing the possible environmental impact of a particular dump of pyritic wastes.

Similarly, although the SPM cannot predict accurately the lifetime of oxidation in the wastes because of the dominance of the effect of oxidation in large particles at the tail end of the oxidation process, the error may be of little practical significance because the sulphate production rate (pollution generation rate) at these times is lower by at least an order of magnitude than the production rate during the first 10–20 years in the lifetime of the oxidation process.

The shapes of the oxygen concentration profile and the heat source distribution profile predicted by the DPM are different from those predicted by the SPM. This is particularly so for the heat source distribution profile. Since both profiles can be measured and used to assess the applicability of the present diffusion model to oxidation in pyritic mine wastes, it is essential to include the particle size distribution in the model.

Acknowledgement

One of the authors (GBD) gratefully acknowledges the Australian Institute of Nuclear Science and Engineering for its financial support through a postgraduate studentship.

Nomenclature

a	particle radius size (m)
a_0	minimum particle radius size in DPM (m)
a_n	maximum particle radius size in DPM (m)
D_1	diffusion coefficient for oxygen in the pore space of the dump (m^2 s^{-1})
D_2	diffusion coefficient for oxygen in water (m^2 s^{-1})
$H(x, t)$	heat source distribution (W m^{-3})
k	$= \gamma(1-p)D_2L^2/D_1a^2$
k_a	$= 0.39k'/(a_n^{0.39} - a_0^{0.39})$
k_H	$= \delta D_1 u_0/\varepsilon L^2$
k'	$= 3a^2k$
L	height of the dump (m)
M	total mass of particle sample (kg)
$M(a)\,da$	mass of particles with radius between a and $a + da$ (kg)
p	porosity of the waste ore (dimensionless)
q^*	rate of loss of oxygen from the pore space (kg m^{-3} s^{-1})
q	$= q^*L^2/D_1u_0$
r^*	radial distance within a particle (m)
R^*	position of the moving reaction front within the particle (m)
R	$= R^*/a$ dimensionless position of reaction front
R_a	found from equation (14)
$S(t)$	integrated sulphate production rate (kg m^{-2} s^{-1})
t^*	time (s)
t	$= t^*/\tau$ dimensionless time
u^*	oxygen concentration within the pore space of the dump (kg m^{-3})

u $= u^*/u_0$ dimensionless oxygen concentration
u_0 concentration of oxygen in air (kg m^{-3})
v^* oxygen concentration within particles of the dump (kg m^{-3})
w defined by equation (15)
x^* vertical spatial coordinate (m)
x $= x^*/L$ dimensionless vertical coordinate
$X(t)$ dimensionless position of planar moving front
γ proportionality constant encompassing both Henry's law and the gas law.
δ heat produced from the oxidation reaction per mass of sulphur oxidized (J kg^{-1})
δ_1 $= pu_0/\varepsilon\rho_s$
δ_s mass of sulphate produced per mass of sulphur consumed by the chemical reaction
ε mass of oxygen consumed per mass of sulphur in the oxidation reaction
v number of particles per unit volume of the dump (m^{-3})
$v(a)\,da$ number of particles per unit volume of the dump whose radii lie between a and $a + da$ (m^{-3})
ρ density of the particulate mass of the dump (kg m^{-3})
ρ_s density of sulphur within the dump (kg m^{-3})
ρ_T overall density of the dump (kg m^{-3})
τ $= L^2\varepsilon\rho_s/D_1u_0$

References

1 Davis, G. B. and Ritchie, A. I. M. A model of oxidation in pyritic mine wastes. I. Equations and approximate solution, *Appl. Math. Modelling*, 1986, **10**, 314–322
2 Davis, G. B., Doherty, G. and Ritchie, A. I. M. A model of oxidation in pyritic mine wastes. II. Comparison of numerical and approximate solutions, *Appl. Math. Modelling*, 1986, **10**, 323–329
3 Ritchie, A. I. M. Heap leaching: A gas diffusion rate-limited model, *AAEC/E429*, 1977
4 Bartlett, R. W. A combined pore diffusion and chalcopyrite dissolution kinetics model for *in situ* leaching of a fragmented copper porphyry, *Int. Symp. on Hydrometallurgy, AIME, New York*, 1973, 331–374
5 Davis, G. B. and Ritchie, A. I. M. A model of pyritic oxidation in waste rock dumps, *Proc. Int. Specialist Conf. on Water Regime in Relation to Milling, Mining and Waste Treatment Including Rehabilitation, with Emphasis on Uranium Mining, Aust. Water and Wastewater Assoc., Darwin*, 1983, **22**(1)–**22**(11)
6 Lewis, A. E. and Braun, R. L. Nuclear chemical mining of primary copper sulphides, *Trans. SME-AIME*, 1973, **254**, 217–224
7 Davis, G. B. and Hill, J. M. A moving boundary problem for the sphere, *IMA J. Appl. Math.*, 1982, **29**, 99–111